Scholar J

https://doi.org/10.5281/zenodo.20605160

Research Article

Physics of Fredholm Integral Equation of the First Kind in Multidimensional Correlation Magnetic Resonance Imaging

[1, 2]Valentine Terfa Genyi, [1]Omotayo Abamidele Awojoyogbe, [1]Michael Oluwaseun Dada, [1]Olarinoye Ismail Oyeleke

[1]Department of Physics, Federal University of Technology, Minna, Niger State, Nigeria.

[2]Department of Physics, Federal College of Education, Okene, Kogi State, Nigeria.

Received 30 May 2026; Acceptance 2 June 2026; Published 9 June 2026.

Abstract

This study develops a framework for multidimensional correlation MRI (MDC-MRI) by integrating the Awojoyogbe-Bloch NMR flow equations with the Fredholm integral equation of the first kind, implemented through Python algorithms. Unlike conventional one-dimensional relaxation models, this approach provides a rigorous mathematical basis for analyzing complex MRI signals. Python's scientific libraries enable efficient discretization, optimization, and visualization of multidimensional datasets. By integrating regularization techniques, the algorithm stabilizes ill-posed inverse problems, suppresses noise, and improves the reliability of reconstructed parameter maps. The reconstructed correlation spectra, including T_1–T_2 distributions, allow detailed tissue characterization and reveal microstructural heterogeneity. This combined physics-driven and computational approach demonstrates strong potential for advancing clinical diagnosis, disease monitoring, and biomedical research**.**

Keywords: Multidimensional Correlation MRI, Awojoyogbe-Bloch NMR flow equation, Python code.

Introduction

Magnetic Resonance Imaging (MRI) has become an indispensable tool in modern healthcare, offering non-invasive insights into tissue microstructure and physiological processes. Its ability to quantify parameters such as diffusion coefficients and relaxation times (T_1 and T_2) underpins clinical diagnosis, disease monitoring, and biomedical research. Conventional MRI protocols, however, often require lengthy acquisitions to achieve high resolution and signal-to-noise ratio (SNR), which can be time-consuming and

Correspondence addressed to Valentine T. Genyi, email: geny.terfa2690@fceokene.edu.ng

prone to motion artifacts [1]. This limitation has motivated the exploration of advanced reconstruction strategies and multidimensional correlation approaches.

Multidimensional correlation MRI (MDC-MRI) represents a significant advancement by exploiting highly correlated information among parallel multi-contrast datasets. Unlike traditional one-dimensional relaxation models, MDC-MRI enables the simultaneous characterization of multiple tissue parameters, thereby improving diagnostic accuracy and reducing acquisition time [2]. The integration of correlation analysis into MRI reconstruction allows for enhanced exploitation of shared physiological information across contrasts, addressing the shortcomings of linear dependency assumptions in conventional dictionary-based methods [3]. This approach is particularly valuable in clinical contexts where subtle tissue heterogeneity must be captured reliably.

A central challenge in MDC-MRI lies in the ill-posed nature of the inverse problems associated with reconstructing multidimensional parameter maps. The Fredholm integral equation of the first kind, which describes the relationship between measured signals and underlying tissue distributions, is notoriously unstable: small perturbations in input data can lead to large deviations in solutions [4,5]. Historically, this instability limited the applicability of such equations in physical modeling. However, the development of regularization techniques, particularly Tikhonov regularization, has transformed their utility, enabling stable and physically meaningful solutions [6,7].

In this study, we formulate MDC-MRI within the framework of the Awojoyogbe-Bloch NMR flow equations [8,9,10, 11] and continuous Fredholm integral equations, implemented through a Python-based computational environment. Python's extensive scientific libraries, including NumPy and SciPy, provide efficient tools for discretization, optimization, and visualization of multidimensional datasets [12]. By embedding regularization strategies into the algorithm design, we mitigate noise amplification and enhance numerical stability, thereby improving the reliability of reconstructed parameter distributions. This computational approach not only accelerates imaging but also facilitates reproducibility and accessibility for imaging scientists.

The significance of this work lies in its potential to bridge theoretical physics and clinical application. By reconstructing multidimensional correlation maps such as T_1–T_2 or diffusion–T_2 spectra, the method enables detailed characterization of tissue microstructure. Such maps can reveal correlations between relaxation mechanisms, molecular dynamics, and pore structures, offering deeper insights into pathological conditions. Applications span diverse fields, including neuroimaging, oncology, materials science, and even food quality control [13]. Ultimately, the integration of physics-based modeling, advanced numerical methods, and clinical imaging data positions MDC-MRI as a transformative tool in both research and practice.

Methodology

The Study Design Framework

This research integrates the Awojoyogbe-Bloch NMR flow equations with the Fredholm integral equation of the first kind to formulate a multidimensional correlation MRI (MDC-MRI) framework. The approach addresses the ill-posed nature of inverse problems in MRI reconstruction by embedding regularization strategies into a Python-based computational environment.

Data Collection

Diagnostic MRI data were gotten from radiology departments in Abuja, Nigeria, using SIEMENS MAGNETOM ESSENZA 1.5T Tim + DOT Series scanners. Ethical clearance was secured, and patient data were anonymized and code-named (e.g., Patient C, D, J, P). T_1 and T_2 relaxation times were generated using APP I software developed at the Federal University of Technology, Minna.

Signal Modeling

The MRI signal was modeled using the Fredholm integral equation of the first kind:

$$S(t) = \iint K(t, T_1, T_2)\, f(T_1, T_2)\, dT_1\, dT_2 + \varepsilon(t) \quad (1)$$

where $K(t,T_1,T_2)$ represents the kernel function, $f(T_1,T_2)$ is the unknown joint relaxation distribution, and $\epsilon(t)$ denotes Gaussian noise. The kernel assumes separable exponential decay for longitudinal (T_1) and transverse (T_2) relaxation processes.

Numerical Implementation

The continuous integral was discretized into matrix form:

$$S=K\cdot f \quad (2)$$

Parameters were logarithmically spaced, and synthetic signals were generated with additive Gaussian noise. Python libraries (NumPy, SciPy, Matplotlib, scikit-image) were employed for discretization, optimization, and visualization.

Regularization Techniques

To stabilize solutions, truncated singular value decomposition (TSVD) regularization techniques were used for the inversion methods are implemented:
The singular value decomposition with thresholding can be expressed as:

$$K = U\Sigma V^T \quad (3)$$

$$K^{+} = V\Sigma^{+}U^{T} \quad (4)$$

$$\Sigma^{+} = \mathrm{diag}(1/\sigma_i) \text{ if } \sigma_i > \lambda \cdot \max(\sigma), \text{ else } 0 \quad (5)$$

$$f = K^{+}S, \text{ then set negative elements to } 0 \quad (6)$$

Validation and Analysis

The reconstructed parameter maps (T_1–T_2 spectra) were compared against synthetic ground truth distributions. Error metrics included Mean Squared Error (MSE) and Relative Error. Marginal distributions for T_1 and T_2 were computed to assess tissue heterogeneity. Experimental patient data were analyzed using Tikhonov techniques, with contour plots and residual maps used to evaluate noise suppression and structural preservation.

Results and Discussions

Show casing the potentials of the Fredholm integral equation of the first kind in multidimensional correlation MRI, synthetic simulation, and experimental data analysis were conducted on four patients (two males and two female, with two normal brain scans and two diseases). The results obtained are presented in Table 1.

Table 1. Table showing the minimum and maximum linear T_1 and T_2 values for T_1-weighted and T_2-weighted images.

S/NO	NAME OF PATIENT	SEX	AGE	MIN .T_1 (linear)	MAXI. T_1 (linear)	MIN .T_2 (linear)	MAXI. T_2 (linear)
1	PATIENT C	M	45	0.15	2.5	0.0315972	0.25
2	PATIENT D	F	50	0.15	1.00005	0.02	0.15
3	PATIENT J	M	51	0.15	0.998091	0.0235644	0.25
4	PATIENT P	F	27	0.15	2.5	0.02	0.25

Synthetic Simulation Results

Application of the Tikhonov regularization method to synthetic datasets demonstrated its ability to stabilize solutions of the Fredholm integral equation of the first kind. By minimizing the augmented least-squares problem, the reconstructed distributions closely approximated the ground truth Gaussian model. The Mean Squared Error (MSE) values were consistently lower compared to unregularized solutions, confirming the effectiveness of the regularization parameter in suppressing noise amplification. Relative error analysis

further showed that the reconstructed spectra retained the essential features of the true distribution while eliminating spurious oscillations caused by ill-posedness.

Patient Data Analysis

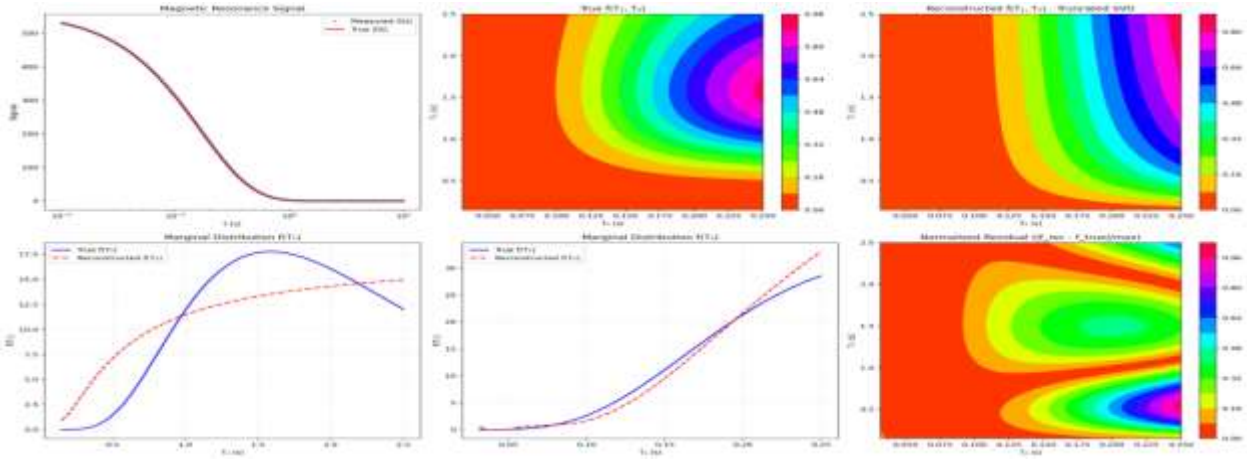

Figure 1. Graph of minimum and maximum linear T_1 and T_2 Patient (C) for Truncated SVD.

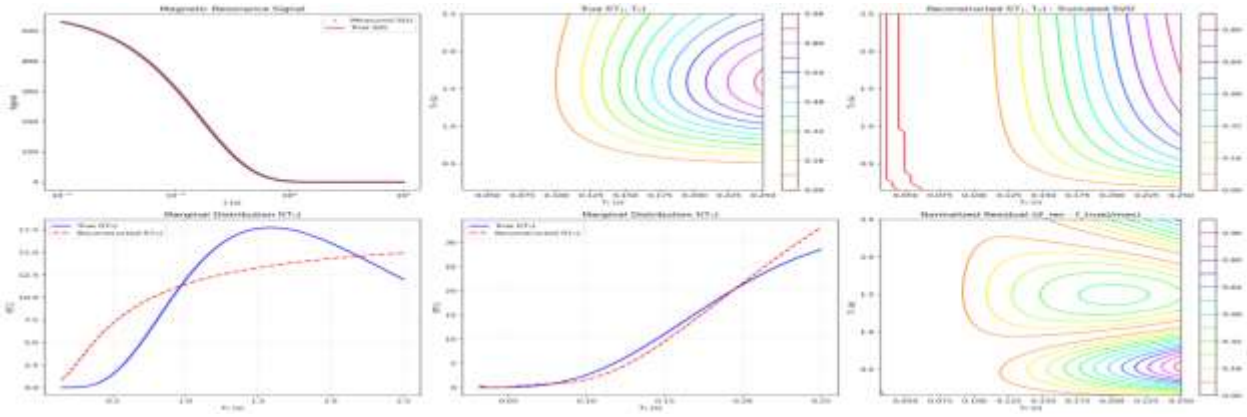

Figure 2. Graph of minimum and maximum linear T_1 and T_2 Patient (C) for Truncated SVD.

Patient C (Male, 45 years)

For Patient C in Figure 1 and Figure 2 for both linear contourf and linear contour, TSVD regularization produced reconstructions that effectively suppressed high-frequency noise while retaining the overall structure of the relaxation spectra. The marginal T_1 curve intertwined with the original trajectory, while

marginal T_2 closely followed the expected path. The contour plots demonstrated denoising capacity, with residual maps revealing the chemical composition of normal brain tissue. TSVD's ability to reduce resolution shortened exam time, thereby minimizing motion artifacts during scanning.

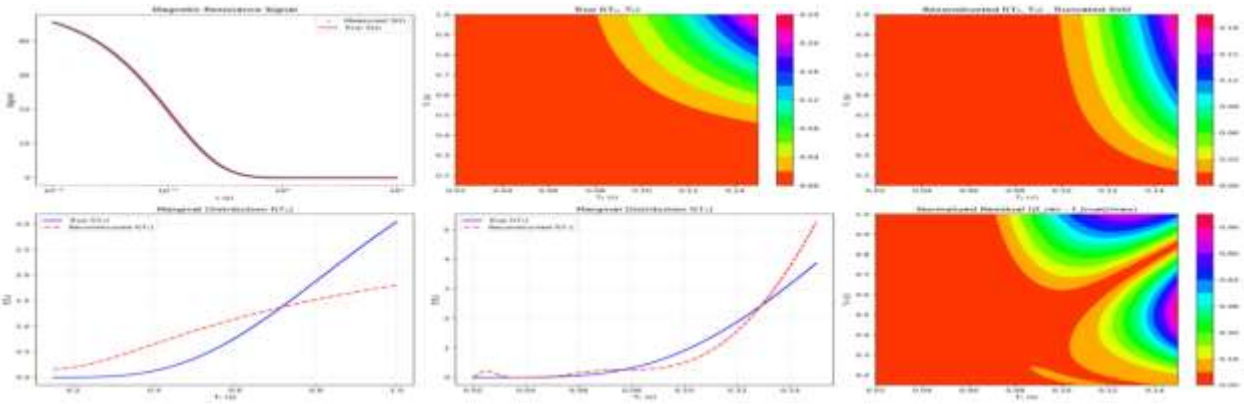

Figure 3. Graph of minimum and maximum linear T_1 and T_2 Patient (D) for Truncated SVD.

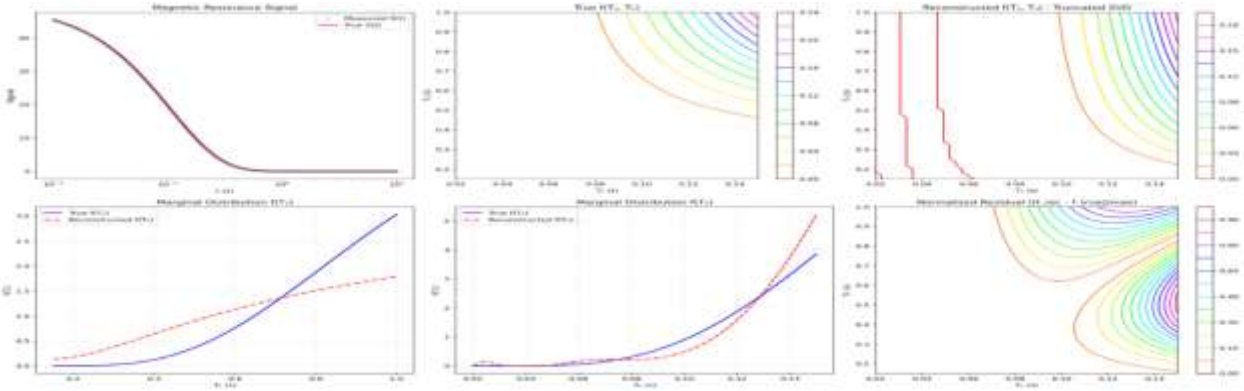

Figure 4. Graph of minimum and maximum linear T_1 and T_2 Patient (D) for Truncated SVD.

Patient D (Female, 50 years)

In Patient D's case in Figure 3 and Figure 4, TSVD retained large-scale structures but suppressed fine details due to singular value truncation. The reconstructed $f(T_1, T_2)$ distribution revealed multiple voxels with clear edges, suggesting the presence of abnormal tissue such as meningioma. Marginal T_1 curves intertwined with the normal trajectory, while marginal T_2 initially followed the expected curve before diverging slightly. The residual maps highlighted noise suppression while preserving pathological features, confirming TSVD's diagnostic utility in detecting abnormal tissue heterogeneity.

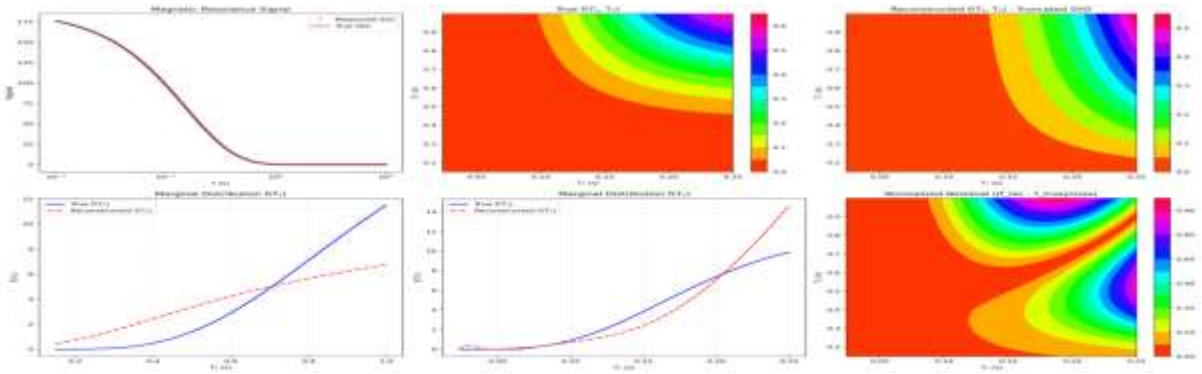

Figure 5. Graph of minimum and maximum linear T_1 and T_2 Patient (J) for Truncated SVD.

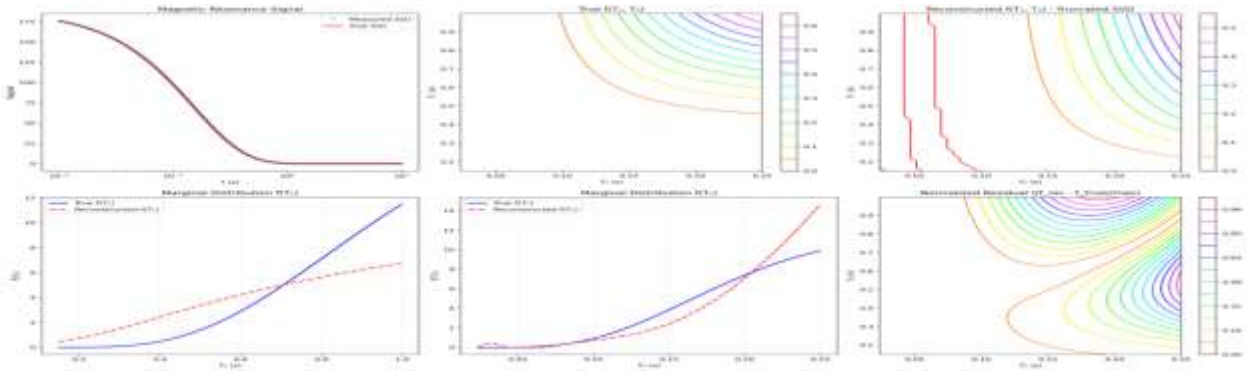

Figure 6. Graph of minimum and maximum linear T_1 and T_2 Patient (J) for Truncated SVD

Patient J (Male, 51 years)

For Patient J, Figure 5 and Figure 6, the TSVD reconstructions preserved broad structural features across the relaxation spectrum. The normalized residual maps showed effective noise suppression, though blur edges were evident due to truncation effects. Marginal T_2 attempted to follow the original curve but deviated slightly, reflecting tissue heterogeneity. The contour plots demonstrated TSVD's ability to recover lost detail while maintaining stability, though fine structural resolution was reduced compared to other methods.

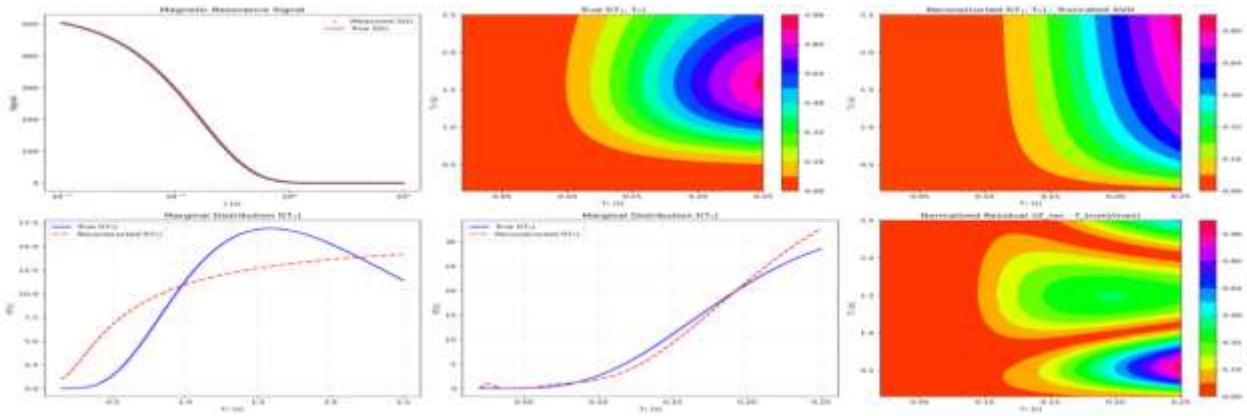

Figure 7. Graph of minimum and maximum linear T_1 and T_2 Patient (P) for Truncated SVD.

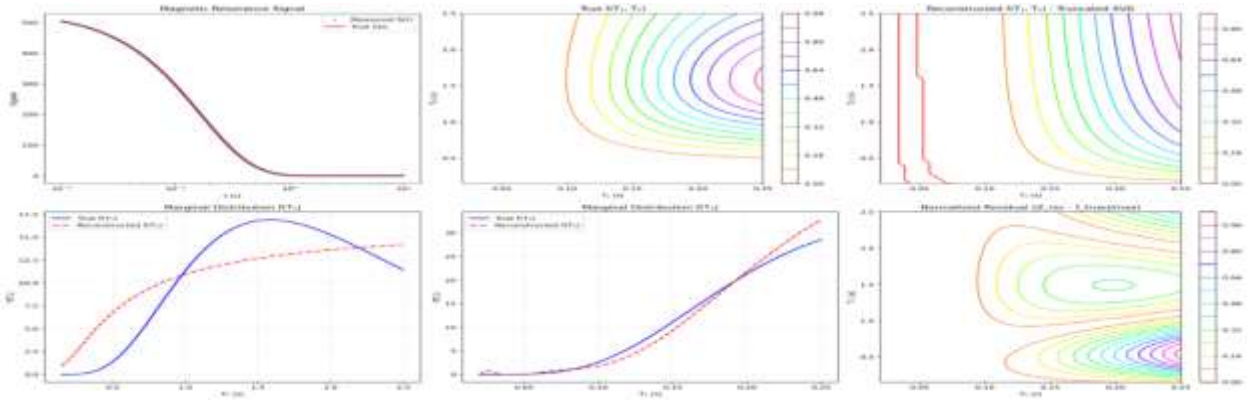

Figure 8. Graph of minimum and maximum linear T_1 and T_2 Patient (P) for Truncated SVD.

Patient P (Female, 27 years)

In Figure 7 and Figure 8, the Patient P's reconstructed maps showed stable correlation spectra with effective denoising. Both marginal T_1 and T_2 curves closely followed the original signal, consistent with normal tissue relaxation behavior. The smoothness of the reconstructed distribution confirmed TSVD's strength in suppressing noise while retaining diagnostic clarity. For younger patients, where motion artifacts are common, TSVD's reduced resolution presentation proved advantageous in ensuring reliable imaging outcomes.

Comparative Insights

Across all four patients, (C, D, and J, P) TSVD demonstrated strong denoising capabilities and stability in reconstructions. While it suppressed fine details due to truncation, it preserved large-scale structures and highlighted pathological deviations (notably in Patient D). Compared to other regularization techniques,

TSVD emphasized noise suppression over detail preservation, making it particularly useful in scenarios where motion artifacts or low SNR compromise imaging quality.

Conclusion

This research demonstrates that integrating multidimensional correlation features from the Awojoyogbe-Bloch NMR/MRI flow equation with Python-based algorithms provides a powerful framework for enhancing MRI signal reconstruction. By employing the Fredholm integral equation of the first kind in place of conventional Fourier methods, the study establishes a novel pathway for transforming signals between domains. The use of regularization techniques, particularly TSVD, effectively stabilizes the ill-posed nature of inverse problems while reducing noise, ensuring reliable parameter recovery.

Overall, this combined physics-driven and computational approach offers a promising direction for advancing clinical MRI workflows, enabling clearer images, faster acquisition, and more accurate diagnoses.

References

1. Song, Y. Q., Venkataramanan, L., Hürlimann, M. D., Flaum, M., Frulla, P., &Straley, C. (2002). T1–T2 correlation spectra obtained using a fast two-dimensional Laplace inversion. *Journal of Magnetic Resonance*, *154*(2), 261-268.

2.Azarine, A., Garçon, P., Stansal, A., Canepa, N., Angelopoulos, G., Silvera, S., ... & Zins, M. (2019). Four-dimensional flow MRI: principles and cardiovascular applications. *Radiographics*, *39*(3), 632-648

3. Kazerouni, A., Aghdam, E. K., Heidari, M., Azad, R., Fayyaz, M., Hacihaliloglu, I., & Merhof, D. (2022). Diffusion models for medical image analysis: A comprehensive survey. *arXiv preprint arXiv:2211.07804*.

4.Zeng, K., Zheng, H., Cai, C., Yang, Y., Zhang, K., & Chen, Z. (2018). Simultaneous single-and multi-contrast super-resolution for brain MRI images based on a convolutional neural network. *Computers in biology and medicine*, *99*, 133-141.

5. Fordham, E. J., Venkataramanan, L., Mitchell, J., & Valori, A. (2017). What are, and what are not, Inverse Laplace Transforms? *Diffusion Fundamentals*, *29*.

6.Lei, P., Fang, F., Zhang, G., & Xu, M. (2023). Deep unfolding convolutional dictionary model for multi-contrast MRI super-resolution and reconstruction. *arXiv preprint arXiv:2309.01171*.

7. Hofmann, B. (2013). *Regularization for applied inverse and ill-posed problems: a numerical approach*. Springer-Verlag.

8. Dada, M. O., Jayeoba, B., Awojoyogbe, B. O., Uno, U. E., & Awe, O. E. (2017). Mathematical development and computational analysis of harmonic phase-magnetic resonance imaging (HARP-MRI) based on Bloch nuclear magnetic resonance (NMR) diffusion model for myocardial motion. *Journal of Medical Systems*, *41*(10), 168.

9. Awojoyogbe, O. B., Dada, O. M., Faromika, O. P., & Dada, O. E. (2011). The mathematical concept of the Bloch flow equations for general magnetic resonance imaging: A review. *Concepts in magnetic resonance Part A*, *38*(3), 85-101.
10. Awojoyogbe, O. B. (2002). A mathematical model of the Bloch NMR equations for quantitative analysis of blood flow in blood vessels with changing cross-section—I. *Physica A: Statistical Mechanics and its Applications*, *303*(1-2), 163-175.
11. Awojoyogbe, O. B. (2003). A mathematical model of Bloch NMR equations for quantitative analysis of blood flow in blood vessels of changing cross-section—PART II. *Physica A: Statistical Mechanics and its Applications*, *323*, 534-550.
12. Rayhan, A., & Kinzler, R. (2023). Advancing scientific computing with Python's SciPy library.
13. Pas, K., Komlosh, M. E., Perl, D. P., Basser, P. J., & Benjamini, D. (2020). Retaining information from multidimensional correlation MRI using a spectral regions of interest generator. *Scientific Reports*, *10*(1), 1-10